Article

Laccase biosensor based on phytic acid modification of nanostructured SiO2 surface for sensitive detection of dopamine

Wenbo Zhao, Kuai Wang, Yuan Wei, Yinghui Ma, Lingling Liu, and Xiaohua Huang

Langmuir, **Just Accepted Manuscript** • DOI: 10.1021/la503104x • Publication Date (Web): 11 Aug 2014

Laccase biosensor based on phytic acid modification of nanostructured SiO_2 surface for sensitive detection of dopamine

Wenbo Zhao*, Kuai Wang, Yuan Wei, Yinghui Ma, Lingling Liu,

and Xiaohua Huang*

National and Local Joint Engineering Research Center of Biomedical Functional Materials, Jiangsu Key Laboratory of Biofunctional Materials, College of Chemistry and Materials Science, Nanjing Normal University, Nanjing 210023, P. R. China.

ABSTRACT: In this work, three kinds of nanostructured silica-phytic acid (SiO_2-PA) materials with diverse morphologies including spherical SiO_2-PA (s-SiO_2-PA), rod-like (r-SiO_2-PA), and helical SiO_2-PA (h-SiO_2-PA) were prepared with the help of electrostatic interaction. The SiO_2-PA nanomaterials with different morphologies were characterized by using transmission electron microscopy (TEM), Fourier transform infrared (FTIR), electrochemical impedance spectroscopy (EIS) and circular dichroism spectrum (CD). Diverse morphologies of SiO_2-PA were used as electrode decorated materials to achieve a high efficiency for electrochemical dopamine (DA) detection. The laccase biosensors were fabricated by immobilizing different morphologies of SiO_2-PA nanomaterials and laccase onto the glassy carbon electrode (GCE) surface, successively. Then the electrochemical responses of the different morphologies of nanostructured SiO_2-PA nanomaterials to laccase were discussed. Results indicated that compared to laccase/s-SiO_2-PA and laccase/r-SiO_2-PA, the laccase/h-SiO_2-PA modified electrode showed the best electrochemical performances.

Keywords: Silica; Biomimetic surface modification; Silica-phytic acid; Laccase;

Biosensor

1. INTRODUCTION

The elegant way for interfacing was offered by electrochemical biosensor at the molecular level. And it also plays a significant role for electronic signal transduction and biological recognition processes[1]. Further, with the development of material science, nanostructured materials (NMs) have wide variety applications in electrochemical biosensors. Many electronic, optical and magnetic functional NMs, which bound to biomolecules (e.g. proteins, peptides, nucleic acids) and used in biosensors, have been developed for detecting and amplifying various signals[2]. Compared to the conventional materials, NMs have obvious advantages in terms of enzymatic immobilization that can attributed to their high surface-to-volume ratios and nanosized-surface activity [3,4].

Recent advances in nanotechnology have led to many different kinds of SiO_2 NMs with a wide variety of highly controlled shapes and sizes[5-7]. The abilities of SiO_2 NMs that offer suitable microenvironment for biomolecules immobilization were investigated by some research groups[8-11]. Many hybrided SiO_2 NMs with conducting materials, such as MWCNT/SiO_2, Au/SiO_2, were also used to prepare nano-biosensors[12,13]. It was proved that these hybrided materials can enhance the efficiency of electrical communication and have the potential act as the substrate for immobilization of biomolecules.

As we all know that the intrinsic properties of NMs mainly depend on their size,

shape, crystallinity, structure, and composition[14]. In this paper, the three kinds of nanostructured silica-phytic acid (SiO_2-PA) materials with diverse morphologies including spherical SiO_2-PA (s-SiO_2-PA), rod-like (r-SiO_2-PA), and helical SiO_2-PA (h-SiO_2-PA) were synthesized and characterized. Laccase was used as the model protein, and the electrochemical responses of the different morphologies nanostructured SiO_2-PA materials to laccase were explored. Further, the direct electrochemistry of these biosensors we proposed for dopamine (DA) was investigated.

2. EXPERIMENTAL SECTION

2.1. Chemical Reagents. Cetyltrimethylammonium bromide (CTAB), triton X-100, hexanol, cicloesano and ammonia aqueous solution ($NH_3 \cdot H_2O$, 71 wt %) were purchased from Lingfeng Chemistry Co. Ltd, China. Tetraethyl orthosilicate (TEOS), hydrochloric acid (HCl) was received from Sinopharm, China. Pluronic F127 (MW=12600 g/mol) was obtained from BASF, Germany. Phytic acid solution (PA, 70 wt%) and its sodium salt hydrate were obtained from Aladdin, China. Laccase (1.34 U/mg) was purchased from Sigma. 3-Hydroxytyramine hydrochloride was purchased from Saen, China. Phosphate buffer solution (PBS) was obtained by self-preparation. Stock solution of laccase (0.3 mg/mL) was made in 0.1 M PBS (pH = 6.0) and kept at 4□.

2.2. Preparation of s-SiO_2-PA, r-SiO_2-PA and h-SiO_2-PA NMs. The three kinds of SiO_2 NMs were synthesized by using two different methods. The spherical SiO_2 NMs were obtained by using a reverse micro-emulsion method as described in the reference[15]. However, both of the rod-like and the helical SiO_2 NMs were easily

prepared by ammonia-catalyzed hydrolysis reaction of TEOS. In these reactions, CTAB and F127 were used as binary templates in acidic aqueous solutions at room temperature[16]. For the synthesis of rod-like and helical SiO_2 NMs, the two procedures were similar except that the volume of CTAB solution was changed. Simple synthesis process is as follows: (1) Synthesis of rod-like and helical SiO_2 NMs. A clear solution was obtained by mixing F127 (0.123 g), CTAB (17.5 mL), concentrated aqueous HCl (4 mL) and H_2O (6.65 mL), and then TEOS (0.425 mL) was added into the above clear solution with agitating. After stirring for 10 s, the mixed solution was kept at 20 ℃ for 20 h, the rod-like SiO_2 NMs were obtained. For the preparation of helical SiO_2-PA NMs, the volume of 0.04 M CTAB solution was 2.5 mL, and other procedures were similar to the synthesis of rod-like NMs. SiO_2 NMs were obtained by centrifugation at 4000 rpm for 15 min, and then washed by ethanol and water, respectively. (2) Synthesis of s-SiO_2-PA, r-SiO_2-PA NMs. Firstly, 0.2 g SiO_2 NMs were added into 80 mL deionized water (DI water), and then 400 μL TEOS was added subsequent for NMs post-coating and surface modification. The solution was then subjected to magnetic stirring for 30 min at room temperature. The active functional groups grafted onto the surface of the SiO_2 NMs were obtained by condensation of TEOS and 400 μL APTES. Then 500 μL PA/PA sodium salt hydrate buffer solution (pH = 7) was dripped into the above solution under stirring. After mixing, the solution was allowed to stir for 24 h. The product was washed with alcohol and DI water, and finally dried at 60□ overnight under vacuum. The amine groups of APTES have positive charges and the phosphate groups of PA have negative charges. So the three kinds of SiO_2-PA NMs were obtained by the help of the electrostatic interaction between phosphate groups and amine on the surface of SiO_2 NMs with different morphologies.

2.3. Preparation of laccase/SiO_2-PA/GCE. Before the modification, the GCE was firstly polished by small alumina powder, and cleaned subsequent by ultra-sonication in ethanol and water bath for 5 min, respectively. After natural drying of the clean GCE, 8.0 μL SiO_2-PA (0.5 mg/mL, various morphologies) were dropped onto the GCE surface and dried naturally. Then 8.0 μL laccase (0.3 mg/mL) was coated onto the SiO_2-PA/GCE surface and stored at 4□. Final, the laccase/SiO_2-PA/GCE was obtained.

2.4. Apparatus and measurements. For obtaining the representative images of transmission electron microscopy (TEM), high-resolution TEM (H-7650, HITACHI Company, Japan) were used. The Fourier transform infrared (FTIR) spectra of different morphologies SiO_2 and SiO_2-PA NMs were measured by FTIR spectrophotometer (Cary 5000, VARIAN Company, USA) with the resolution is 4 cm^{-1}. The far-UV circular dichroism (CD) spectra were measured by CD spectrophotometer (Chirascan, Applied Photophysics Company, UK). The contents of various conformations of laccase were analyzed and calculated by the help of the JASCO710 program.

All electrochemical tests were carried out and analyzed by electrochemical analyzer (760C, CHI Instruments, Inc., US). For cyclic voltammogram experiments, the scan range of the electrodes was from -0.4 to 0.8 V with a scan rate of 100 $mV \cdot s^{-1}$, and prior to the electrochemical experiments, the solution were deoxygenated by high purity nitrogen. Electrochemical impedance spectroscopy (EIS) was performed in a KCl solution (0.1 M) containing 5 mM $K_3Fe(CN)_6$ and 5 mM $K_4Fe(CN)_6$. The current-time curves of oxidation of DA were investigated with an operating potential of +0.22 V.

3. RESULTS AND DISCUSSION

3.1. Characterization of the SiO_2-PA NMs. Fig. 1 showed the TEM images and size distribution of SiO_2-PA NMs with different morphologies. The s-SiO_2-PA NMs were consisted of extremely monodispersed nanoparticles having an average primary particle size of 50 nm (Fig. 1a). The r-SiO_2-PA NMs were nearly monodisperse with the average length of 300 nm and diameter of 100 nm (Fig. 1b). As to the h-SiO_2-PA NMs, their helical shapes with lengths up to several micrometers and the average diameter of 50 nm can be observed (Fig. 1c).

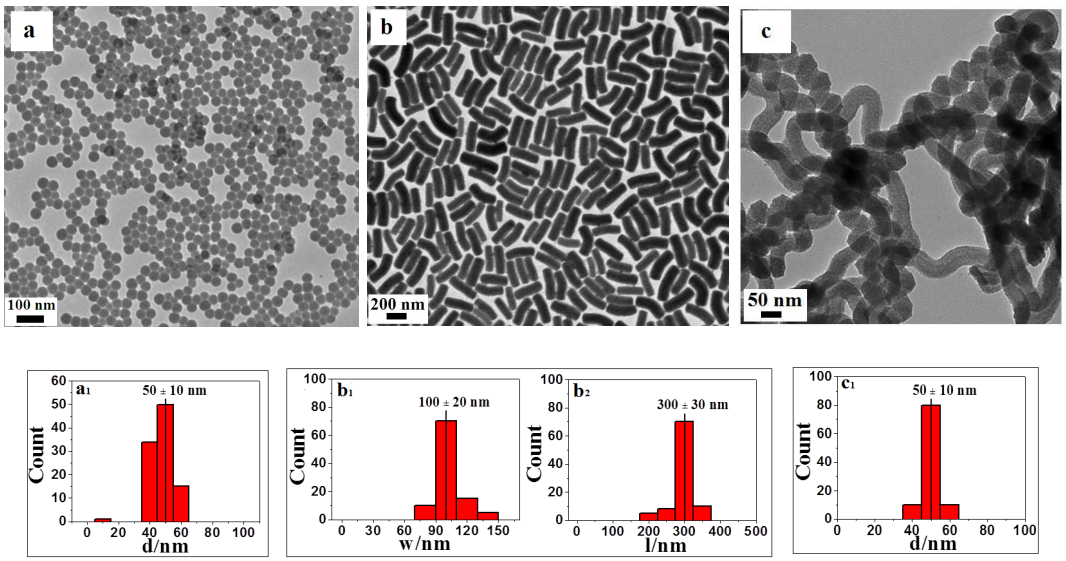

Figure 1. (up) TEM images of s-SiO_2-PA (a), r-SiO_2-PA (b) and h-SiO_2-PA (c). (down) And histogram of the diameter (a_1) distribution of s-SiO_2-PA, the width (b_1) and length (b_2) distribution of r-SiO_2-PA, and the diameter (c_1) distribution of h-SiO_2-PA obtained from TEM images of the nanomaterials.

The FTIR spectra of the three kinds of SiO_2 and SiO_2-PA NMs were represented in Fig. 2 with the resolution is 4 cm^{-1}. The spectrum of SiO_2 showed two bands around

973 and 1110 cm^{-1}, which were attributed to asymmetric O–Si–O stretching (curve a of Fig. 2A, 2B and 2C)[17]. In the spectrum of SiO_2-PA, the speaks at 2927, 1560 and 693 cm^{-1} were attributed to –C–NH_2 stretching, symmetric –NH_2 stretching and the bending vibrations of –NH, respectively (curve b of Fig. 2A, 2B and 2C). Results indicated APTES was grafted onto the surface of SiO_2 successfully. Further, the intensity of the peak at 1104 cm^{-1} increased because of the phosphate bands of PA and the overlap of this phosphate bands with the O–Si–O bands[18]. It meant that PA was successfully modified the surface of SiO_2 NMs by the help of electrostatic interaction. PA, known as inositol hexakisphosphate, is obtained from beans, cereal grains, and animal hematids. Its salts have strong electrostatic interaction that attributed to its small molecules with six phosphate groups. So it can easy form stable films with positive polyelectrolytes[19,20].

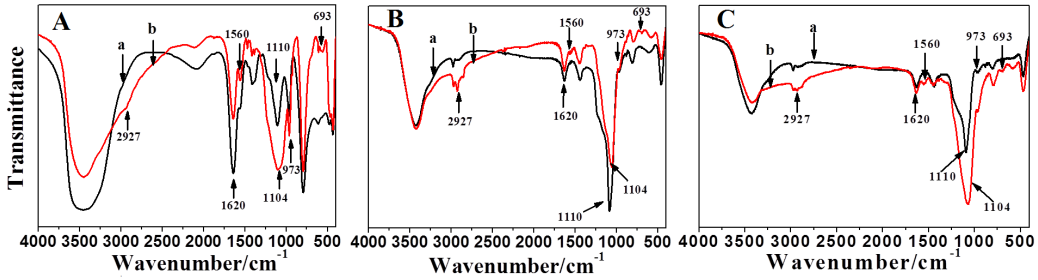

Figure 2. (A) FTIR of (a) s-SiO_2 and (b) s-SiO_2-PA; (B) FTIR of (a) r-SiO_2 and (b) r-SiO_2-PA; (C) FTIR of (a) h-SiO_2 and (b) h-SiO_2-PA.

The conductivities of bare GCE, s-SiO_2/GCE, r-SiO_2/GCE, h-SiO_2/GCE, s-SiO_2-PA/GCE, r-SiO_2-PA/GCE and h-SiO_2-PA/GCE were investigated by EIS (Fig. 3). This program can exhibit the electrochemical impedance status of electrode surface we prepared. The semicircle portion of the Nyquist plot, corresponded to the electron-transfer limited process, was measured at higher frequencies. And the linear portion of the Nyquist plot was obtained at lower frequencies. It corresponds to the

impedance of diffusion process of the electrode reaction. The charge transfer resistance (R_{ct}), equaled to the semicircle diameter, was used to describe the interface properties of electrode[21,22]. For the EIS of the bare GCE (Fig. 3A, curve a), the semicircle domain on EIS was very small. It indicated there was a very low R_{ct} to the redox-probe that dissolved in our electrolyte solution. All of the R_{ct} values (Fig. 3A) of the s-SiO_2/GCE (curve b), r-SiO_2/GCE (curve c) and h-SiO_2/GCE (curve d) were larger than that data of the bare GCE. It indicated that the SiO_2 layer coated onto the GCE surface really inhibited the electron transfer efficiency of the redox-probe of $[Fe(CN)_6]^{3-/4-}$ to the GCE surface. However, all of the R_{ct} value of the s-SiO_2-PA/GCE (curve e), r-SiO_2-PA/GCE (curve f) and h-SiO_2-PA/GCE (curve g) were much less than that of s-SiO_2/GCE (curve b), r-SiO_2/GCE (curve c) and h-SiO_2/GCE (curve d) obviously. Results indicated that the modified PA layer was in favor of the electron transfer between $[Fe(CN)_6]^{3-/4-}$ and the GCE surface. It should be noted that the equivalent circuit model was inserted in Fig. 3A. It represented the typical electrochemical interface that used to fit the impedance data into R_{ct} values.

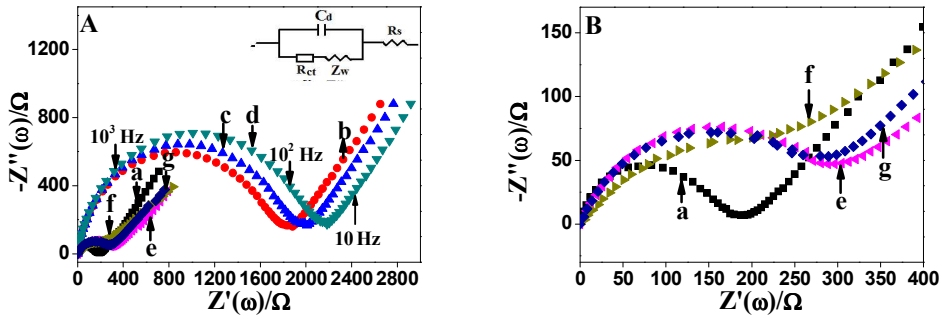

Figure 3. (A) EIS in 0.1 M KCl that containing 0.5 mM $K_3Fe(CN)_6/K_4Fe(CN)_6$, bare (a), s-SiO_2 (b); r-SiO_2 (c); h-SiO_2 (d); s-SiO_2-PA (e); r-SiO_2-PA (f) and h-SiO_2-PA (g) modified GCE electrode. The frequencies swept from 10^4 to 10^{-1} Hz at the formal potential of the redox couple. The three characteristic frequencies of the main semicircles were marked in curve e. Inset of (A): schematic of equivalent circuit. (B)

Close-up of plots (a), (e), (f) and (g).

Circular dichroism (CD) spectroscopy was used extensively over the past few decades to investigate of the secondary structure of biomolecules[23]. CD acted as an attractive analytical tool that attributed to its speed, sensitivity and special capability of analyzing surface-adsorbed. Here, the influence of SiO_2-PA NMs on the secondary structure of laccase was investigated by CD technique. To account for the structural variation of laccase in the PBS (pH = 6.0) with changing morphologies of SiO_2-PA, the far-UV CD spectra were recorded (Fig. 4A). The major negative band (215 nm) and positive band (195 nm) of CD spectra were attributed to the n–π* and the π–π* amide transitions, respectively[24]. Bands of laccase/s-SiO_2-PA (Fig. 4A-b), laccase/r-SiO_2-PA (Fig. 4A-c) and laccase/h-SiO_2 (Fig. 4A-d) looked almost the same as that of pure laccase (Fig. 4A-a). There were just slight increases for the intensity of the two bands (195 nm and 215 nm). It indicated that there was not obviously changed for the secondary structure of laccase. At the same time, the secondary structural elements of laccase were calculated from CD data by using CDNN program (Fig. 4B). The data demonstrated that the native conformation of laccase (pure) contained ~28.3% α-helices, ~20% β-sheets, ~17.7% β-turns, and ~35.8% random coils. Compared to pure laccase, the slightly increase of the a-helix structure (s: ~29.5%, r: ~29.4%, h: ~30.1%) and a little bit loss of β-sheet (s: ~19.2%, r: ~19.3%, h: ~18.8%), β-turn (s: ~17.5%, r: ~17.5%, h: ~17.3%) and random coil (s: ~34.7%, r: ~35.0%, h: ~34.3%) were observed when pure laccase contacted with SiO_2-PA NMs. Here, results of CD spectra can be used to explain the reason why the laccase still remained good catalytic activity in the presentence of SiO_2-PA NMs. It was very important for the performance of biosensor[25-28].

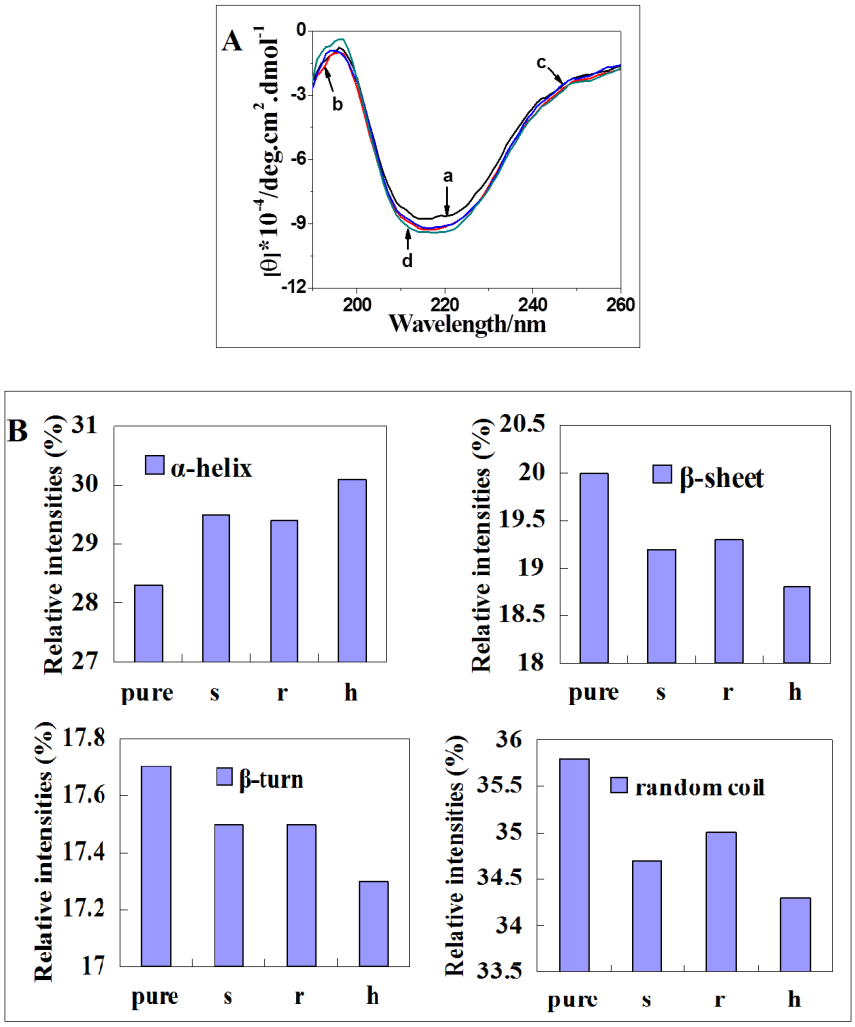

Figure 4. (A) The CD spectra of pure laccase (a); laccase/(s-SiO_2-PA) (b); laccase/(r-SiO_2-PA) (c) and laccase/(h-SiO_2-PA) (d) in 0.1 M PBS (pH = 6.0) in the 190-260 nm wavelength region. (B) Relative amounts of native conformations in pure laccase and s-SiO_2-PA (s) r-SiO_2-PA (r) and h-SiO_2-PA (h) bioconjugate system (0.3 mg/mL laccase and 50 μg/mLSiO_2-PA) in 0.1 M PBS (pH = 6.0). The data were obtained from CD spectra by using the CDNN program.

3.2. Direct electrochemistry of the laccase/(SiO_2-PA)/GCE. The laccase/(SiO_2-PA)/GCE biosensor toward the oxidation of DA can be affected by a variety of parameters[29,30]. The properties of different morphologies SiO_2-PA modified

GCE were studied by using cyclic voltammetry method. As shown in Fig. 5 for GCE (curve a) and laccase/GCE (curve b), no redox response could be observed in the potential range from -0.4 to +0.8 V. It indicated that the laccase was not well fixed on the electrode surface in the absence of suitable nanomaterials. But all of the laccase/s-SiO_2-PA/GCE (curve c), laccase/r-SiO_2-PA/GCE (curve d) and laccase/h-SiO_2-PA/GCE (curve e) exhibited the CV peaks with a formal potential value of +0.22 V. Compared with laccase/s-SiO_2-PA/GCE (I_p = 1.392 μA) and laccase/r-SiO_2-PA/GCE (I_p = 0.1183 μA), laccase/h-SiO_2-PA/GCE (I_p = 2.608 μA) showed higher oxidation peak currents. A smaller current to laccase/r-SiO_2-PA/GCE was observed because r-SiO_2-PA had a larger R_{ct}, which agreed well with the analysis results obtained from EIS. The waves appearing with higher intensity of h-SiO_2-PA NMs included the following traits: firstly, the decorated nanomaterials were in favor of more enzymes fixed onto electrode surface[31]. Secondly, the laccase attached to the h-SiO_2-PA film surface had more spatial freedom in its orientation. So it facilitated the direct electron transfer[32]. Finally, h-SiO_2-PA had special helix structure, and can combine with more laccase. Therefore, h-SiO_2-PA was selected as the optimal decorated substrate to immobilize laccase for detecting DA in three kinds of SiO_2-PA NMs.

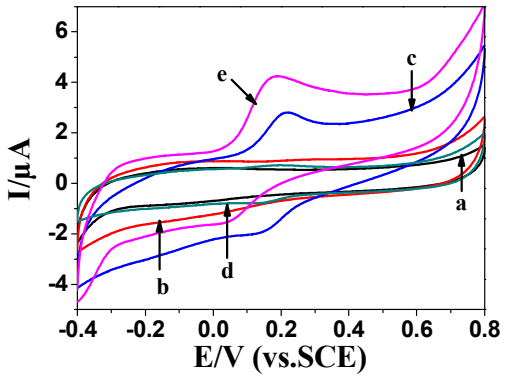

Figure 5. Cyclic votammograms of GCE (a); laccase/GCE (b); laccase/(s-SiO_2-PA)

(c); laccase/(r-SiO_2-PA) (d) and laccase/(h-SiO_2-PA) (e) in PBS (0.1 M, pH = 6.0) containing 5 μM DA with a scan rate of 100 $mV \cdot s^{-1}$.

The working principle of this biosensor was as follows: DA was oxidized to its corresponding dopamine-o-quinone (DOQ) by laccase (oxid)/SiO_2-PA modified electrode, and then laccase (red) lost electrons to form laccase (oxid). Thus, it formed a bioelectrocatalytic cycle and thereby generated electrons, which were passed to working electrode (Scheme 1)[33,34].

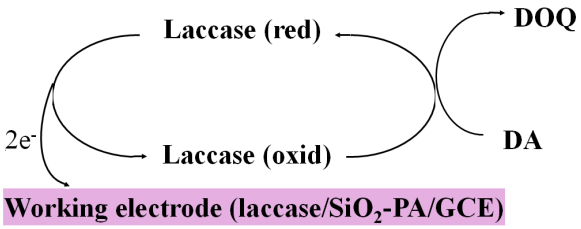

Scheme 1. Chemical reaction mechanisms for direct electrocatalysis of DA by laccase/SiO_2-PA/GCE.

3.3. Amperometric response of DA at laccase biosensor. The amperometric responses of the laccase/(s-SiO_2-PA) (Fig. 6A-a), laccase/(r-SiO_2-PA) (Fig. 6A-b) and laccase/(h-SiO_2-PA) (Fig. 6A-c) modified GCE were investigated with the successive addition of DA at an applied potential of +0.22 V. The above biosensors exhibited different responses to the change of DA concentration. Compared with laccase/(s-SiO_2-PA)/GCE (Fig. 6A-a and Fig. 6B-a) and laccase/(r-SiO_2-PA)/GCE (Fig. 6A-b and Fig. 6B-b), laccase/(h-SiO_2-PA)/GCE exhibited higher sensitivity and lower detection limit. The calibration plot resulting from current-time response of laccase/(h-SiO_2-PA)/GCE was presented in Fig. 6B (curve c). With the increasing DA

concentration in a range from 0.99 to 138.40 μM, the peak current of catalytic oxidation was simultaneously increased linearly. The linear regression equation was [I_p/μA = (4.44 ± 0.004) × 10^{-2}/μA + (1.66 ± 0.002) × 10^{-3} [DA]/μM] (R^2 = 0.9992), and the detection limit was 0.17 (± 0.002) μM, which was calculated from the ratio of signal to noise ratio (S/N) of 3. This datum was lower than most previously published reports (Table 1)[35-38].

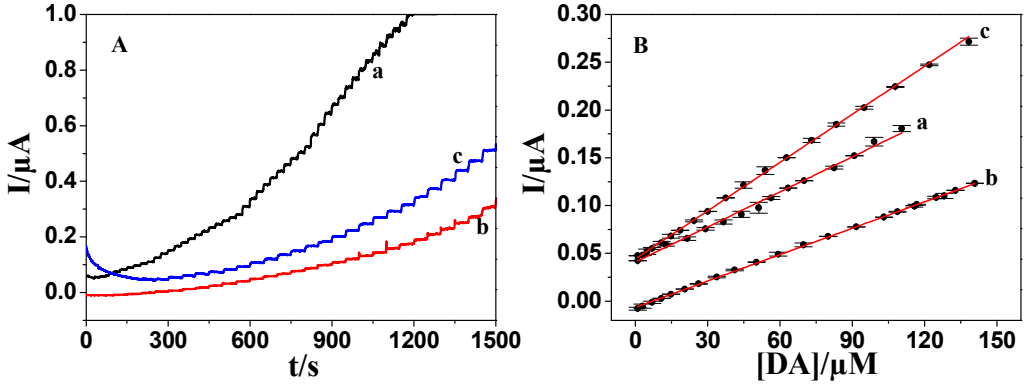

Figure 6. (A) Current-time response of laccase/(s-SiO_2-PA)/GCE (a), laccase/(r-SiO_2-PA)/GCE (b) and laccase/(h-SiO_2-PA)/GCE (c) by successive additions of DA in a 0.1 M PBS (pH = 6.0) at applied potential +0.22 V. (B) Calibration plots obtained for laccase/(s-SiO_2-PA)/GCE (a), laccase/(r-SiO_2-PA)/GCE (b) and laccase/(h-SiO_2-PA)/GCE for DA detection.

Table 1. Comparison of a few reported values for detection limit, linear range and R-square of DA.

Biosensor	Detection limit (μM)	Linear range(μM)	R-square	Ref.
Laccase/Si/MWCNTs/SPE	0.42	1.3-85.5	0.991	33
Laccase/MWNT-based	0.4	10-30	0.974	34
TGA-capped CdTe QD/Lac	0.16	0.3-100	0.996	35

Bean sprout/SAM/Au	0.48	9.91-221	0.999	36
MAO/GCE	20.00	50-250	0.987	37
Laccase/(h-SiO_2-PA)/GCE	0.17	0.99-138.40	0.999	This work

The repeatability of the biosensor we proposed was studied by using five independently prepared biosensors at the DA concentration of 10 μM. Results showed that the resulting relative standard deviations of five times measurements were less than 5%, and indicated the biosensor had good reproducibility. Further, the electrode was stored in dry, closed environment, and was detected in the PBS solution. After 20 days, the enzyme electrode still kept 89% of its initial activity.

3.4. Anti-interferences of laccase/(h-SiO_2-PA)/GCE biosensor. Some substances in real samples such as glucose (Glu), ascorbic acid (AA), uric acid (UA), and etc., may affect the electrochemical detection of analyte[39]. In this case, the anti-interference abilities of the laccase/(h-SiO_2-PA)/GCE were investigated. The differential pulse voltammetry responses of analyzed solutions containing DA and mixture of DA and different electroactive species (such as Glu, phenol (Phe), cysteine (Cys), nonylphenol (NP), UA and AA) were recorded and analyzed, respectively. The influences of Glu, Phe, Cys, AA, NP and UA on the electrochemical detection of DA were presented in Fig. 7. The results showed that the responses of DA and the mixture of DA with electroactive species were similar, and indicated that the biosensor we proposed had a good anti-interference ability.

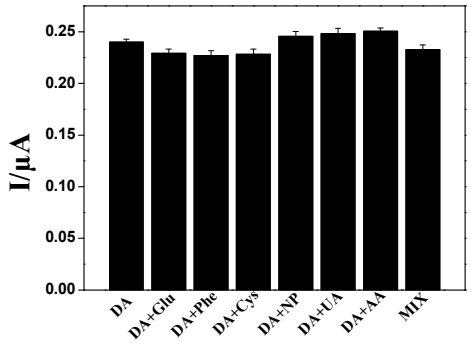

Figure 7. Amperometric responses of the laccase/(h-SiO_2-PA)/GCE biosensor upon additions of DA (3 μM), and a mixture of DA (3 μM) and electroactive species (Glu (1 mM), Phe (1 mM), Cys (1 mM), NP (1 mM), UA (100 μM) and AA (50 μM)) in PBS, respectively. MIX was a mixture of DA (3 μM) with all electroactive species in PBS.

3.5. Real sample analysis. Pharmaceutical injection samples and rabbit blood serums were chosen as models for evaluating the practical utility of the laccase/(h-SiO_2-PA)/GCE biosensor we proposed. Fresh blood sample (obtained from anticoagulated rabbit whole blood) was collected and centrifuged at 3000 rpm. After 5 min, the supernatant liquid (serum) was obtained and separated for next step. As far as we know, there was no standard procedure for the determination of DA concentration in rabbit blood serum, so the recovery testing was used to evaluating the practical utility of the laccase/(h-SiO_2-PA)/GCE biosensor[40-42]. The DA analytic recoveries of target sample (pharmaceutical injection or rabbit blood serum) were determined by the proposed biosensor.

Before detection, the models including pharmaceutical and serum samples were

diluted with PBS, and certain amounts of DA were then added, respectively. The analytical results were shown in Table 2. The average recovery of DA concentration was 98.55%. Further, the comparison between the experimental data and the results of previous references (Control sample 1-3) indicated the recoveries were acceptable[40-42].

Table 2. Recovery tests for detection of DA of real samples (n = 3).

Sample	DA/μM added	DA/μM found	Recovery (%)	Ref
	2.00	1.98	99.00%	
Pharmaceutical injection samples	13.00	14.28	94.46%	
	30.00	32.91	102.84%	This work
	10	9.93	99.30%	
Rabbit blood serum samples	30	29.49	98.30%	
	50	48.71	97.42%	This work
Control sample 1	(2.00 ~ 6.00)	(1.91 ~ 5.899)	(97.50 ~ 103.00)	40
Control sample 2	(0.2 ~ 10)	(0.28 ~ 15.33)	(93.33 ~ 103.53)	41
Control sample 3	(1.2 ~ 3.7)	(1.3 ~ 3.8)	(98 ~ 102)	42

4. CONCLUSION

In this case, the effects of different morphologies of SiO_2-PA on the performances of amperometric laccase biosensor we prepared were investigated. Results showed that laccase adsorbed onto h-SiO_2-PA NMs had the best electrochemical performances. The biosensor based on laccase immobilized onto h-SiO_2-PA possessed many advantages including high enzymatic activity, low detection limit, short response time, satisfactory anti-interference ability and selectivity. Therefore, h-SiO_2-PA NMs were recommended as decorated material of electrode of enzyme-based biosensor, and the

related mechanism of proposed applications will be further investigated as well. It is expected that this convenient fabrication of enzyme devices would be useful in the development of clinical detection.

■ AUTHOR INFORMATION

Corresponding Author

*E-mail:zhaowenbo@njnu.edu.cn (W. Zhao); huangxiaohua_njnu@163.com (X. Huang).

*Phone: +86 25 85891536; fax: +86 25 83598280.

Notes

The authors declare no competing financial interest.

■ ACKNOWLEDGMENTS

This work was supported by Jiangsu Collaborative Innovation Center of Biomedical Functional Materials, Base of Natural Science Foundation of Jiangsu Province of China (BK 20131396), Natural Science Foundation of Universities of Jiangsu Province (14KJA150006), production, education & research of prospective joint research project of Jiangsu Province (BY2011109).

■ REFERENCES

1. Wang, J. Nanomaterial-based electrochemical biosensors. *Analyst* **2005,** *130*,

421-426.

2. Chen, J. R.; Miao, Y. Q.; He, N. Y.; Wu, X. H.; Li, S. J. Nanotechnology and biosensors. *Biotechnol. Adv.* **2004,** *22*, 505-518.

3. Zhao, Z.; Lei, W.; Zhang, X.; Wang, B.; Jiang, H. ZnO-based amperometric enzyme biosensors. *Sensors* **2010,** *10*, 1216-1231.

4. Tian, Z. R.; Voigt, J. A.; Liu, J.; Mckenzie, B.; Mcdermott, M. J. Biomimetic arrays of oriented helical ZnO nanorods and columns. *J. Am. Chem. Soc.,* **2002,** *124*, 12954-12955.

5. Lin, H. P.; Mou, C. Y. Structural and morphological control of cationic surfactant-templated mesoporous silica. *Acc. Chem. Res.* **2002,** *35*, 927-935.

6. Wan, Y.; Zhao, D. On the controllable soft-templating approach to mesoporous silicates. *Chem. Rev.* **2007,** *107*, 2821-2860.

7. Yang, Z.; Lu, Y.; Yang, Z. Mesoporous materials: tunable structure, morphology and composition. *Chem. Commun.* **2009**, *17*, 2270-2277.

8. Collings, A.; Caruso, F. Biosensors: recent advances. *Rep. Prog. Phys.* **1997,** *60*, 1397-1445.

9. Tripathi, V. S.; Kandimalla, V. B.; Ju, H. Preparation of ormosil and its applications in the immobilizing biomolecules. *Sens. Actuat. B* **2006,** *114*, 1071-1082.

10. Qhobosheane, M.; Santra, S.; Zhang, P.; Tan, W. Biochemically functionalized silica nanoparticles. *Analyst* **2001,** *126*, 1274-1278.

11. Yang, H.; Zhu, Y. A high performance glucose biosensor enhanced via nanosized SiO_2. *Anal. Chim. Acta* **2005,** *554*, 92-97.

12. Gopalan, A. I.; Lee, K. P.; Ragupathy, D.; Lee, S. H.; Lee, J. W. An electrochemical glucose biosensor exploiting a polyaniline grafted multiwalled carbon nanotube/perfluorosulfonate ionomer-silica nanocomposite. *Biomaterials* **2009,** *30*, 5999-6005.

13. Bai, Y.; Yang, H.; Yang, W.; Li, Y.; Sun, C. Gold nanoparticles-mesoporous silica composite used as an enzyme immobilization matrix for amperometric glucose biosensor construction. *Sens. Actuat. B* **2007,** *124*, 179-186.

14. Mao, C.; Chen, X. B.; Hou, X. M.; Shen, J.; Zhu, J. J.; Zhao, W. B. Synthesis of rambutan-like hybrid nanospheres of Au-P123. *Gold Bull.* **2009**, 42, 215-218.

15. Bagwe, R. P.; Hilliard, L. R.; Tan, W. Surface modification of silica nanoparticles to reduce aggregation and nonspecific binding. *Langmuir* **2006,** *22*, 4357-4362.

16. Ye, J.; Zhang, H.; Yang, R.; Li, X.; Qi, L. Morphology-controlled synthesis of SnO_2 nanotubes by using 1D silica mesostructures as sacrificial templates and their applications in lithium-ion batteries. *Small* **2010,** *6*, 296-306.

17. Hsiao, V. K.; Waldeisen, J. R.; Zheng, Y.; Lloyd, P. F.; Bunning, T. J.; Huang, T. J. Aminopropyltriethoxysilane (APTES)-functionalized nanoporous polymeric gratings: fabrication and application in biosensing. *J. Mater. Chem.* **2007,** *17*, 4896-4901.

18. Zhao, W.; Ni, Y.; Zhu, Q.; Fu, R.; Huang, X.; Shen, J. Innovative biocompatible nanospheres as biomimetic platform for electrochemical glucose biosensor. *Biosens. Bioelectron.* **2013,** *44*, 1-5.

19. Tang, F.; Wang, X.; Xu, X.; Li, L. Phytic acid doped nanoparticles for green anticorrosion coatings. *Colloid. Surf. A* **2010,** *369*, 101-105.

20. McKenzie, K. J.; Marken, F.; Opallo, M. TiO_2 phytate films as hosts and conduits for cytochrome c electrochemistry. *Bioelectrochemistry* **2005,** *66*, 41-47.

21. Ye, P.; Xu, Z. K.; Wu, J.; Innocent, C.; Seta, P. Nanofibrous poly(acrylonitrile-co-maleic acid) membranes functionalized with gelatin and chitosan for lipase immobilization. *Biomaterials* **2006,** *27*, 4169-4176.

22. Mequanint, K.; Patel, A.; Bezuidenhout, D. Synthesis, Swelling Behavior, and Biocompatibility of Novel Physically Cross-Linked Polyurethane-block-Poly (glycerol methacrylate) Hydrogels. *Biomacromolecules* **2006,** *7*, 883-891.

23. Fears, K. P.; Sivaraman, B.; Powell, G. L.; Wu, Y.; Latour, R. A. Probing the conformation and orientation of adsorbed enzymes using side-chain modification. *Langmuir* **2009,** *25*, 9319-9327.

24. Bonomo, R.; Cennamo, G.; Purrello, R.; Santoro, A.; Zappala, R. Comparison of three fungal laccases from Rigidoporus lignosus and Pleurotus ostreatus: correlation between conformation changes and catalytic activity. *J. Inorg. Biochem.* **2001,** *83*, 67-75.

25. Solanki, P. R.; Kaushik, A.; Agrawal, V. V.; Malhotra, B. D. Nanostructured metal oxide-based biosensors. *NPG Asia Mater.* **2011**, 3, 17-24.

26. Sun, C.; Chen, L. B.; Xu, F.; Zhu, P. Y.; Luan, J. F.; Mao, C.; Shen, J. Hemocompatible and antibiofouling PU-F127 nanospheres platform for application to glucose detection in whole blood. *J. Mater. Chem. B* **2013**, 1, 801-809.

27. Kaushik, A.; Khan, R.; Solanki, P. R.; Pandey, P.; Alam, J.; Ahmad, S.; Malhotra, B. D. Iron oxide nanoparticles-chitosan composite based glucose biosensor. *Biosens.*

Bioelectron. **2008**, 24, 676-683.

28. Pandey, P.; Datta, M.; Malhotra, B. D. Prospects of nanomaterials in biosensors. *Anal. Lett.* **2008**, 41, 159-209.

29. Zhu, Q.; Sun, C.; Yan, J.; Yang, K.; Fu, R.; Mao, C.; Shen, J. Facile Fabrication of Au-F127 Nanocolloids with Different Morphologies and their Potential Bioapplications. *Aust. J. Chem.* **2013,** *66*, 381-390.

30. Zhai, Y.; Zhai, S.; Chen, G.; Zhang, K.; Yue, Q.; Wang, L.; Liu, J.; Jia, J. Effects of morphology of nanostructured ZnO on direct electrochemistry and biosensing properties of glucose oxidase. *J. Electroanal. Chem.* **2011,** *656*, 198-205.

31. Zhao, Y.; Jiang, Z.; Lin, D.; Dong, A.; Li, Z.; Wu, H. Enhanced proton conductivity of the proton exchange membranes by the phosphorylated silica submicrospheres. *J. Power Sources* **2013,** *224*, 28-36.

32. Zhang, G.; Yang, N.; Ni, Y.; Shen, J.; Zhao, W.; Huang, X. A H_2O_2 electrochemical biosensor based on biocompatible PNIPAM-g-P(NIPAM-co-St) nanoparticles and multi-walled carbon nanotubes modified glass carbon electrode. *Sens. Actuat. B* **2011,** *158*, 130-137.

33. Rawal, R.; Chawla, S.; Pundir, C. S. Polyphenol biosensor based on laccase immobilized onto silver nanoparticles/multiwalled carbon nanotube/polyaniline gold electrode. *Anal. Biochem.* **2011,** *419*, 196-204.

34. Xiang, L.; Lin, Y.; Yu, P.; Su, L.; Mao, L. Laccase-catalyzed oxidation and intramolecular cyclization of dopamine: A new method for selective determination of dopamine with laccase/carbon nanotube-based electrochemical biosensors.

Electrochim. Acta **2007,** *52*, 4144-4152.

35. HabibáKazemi, S. A novel quantum dot-laccase hybrid nanobiosensor for low level determination of dopamine. *Analyst* **2012,** *137*, 5553-5559.

36. Li, Y.; Zhang, L.; Li, M.; Pan, Z.; Li, D. A disposable biosensor based on immobilization of laccase with silica spheres on the MWCNTs-doped screen-printed electrode. *Chem. Cent. J.* **2012,** *6*, 1-8.

37. Moccelini, S. K.; Fernandes, S. C.; Vieira, I. C. Bean sprout peroxidase biosensor based on l-cysteine self-assembled monolayer for the determination of dopamine. *Sens. Actuat. B* **2008,** *133*, 364-369.

38. Joshi, P.; Joshi, H. C.; Sanghi, S. K.; Kundu, S. Immobilization of monoamine oxidase on eggshell membrane and its application in designing an amperometric biosensor for dopamine. *Microchim. Acta* **2010,** *169*, 383-388.

39. Zhang, J.; Lei, J.; Pan, R.; Xue, Y.; Ju, H. Highly sensitive electrocatalytic biosensing of hypoxanthine based on functionalization of graphene sheets with water-soluble conducting graft copolymer. *Biosens. Bioelectron.* **2010,** *26*, 371-376.

40. Zhou, Y. Z.; Zhang, H. Y.; Zhang, J.; Liu, T.; Tang, W. M. Electrochemically sensitive determination of dopamine and uric acid based on poly (beryllon II)/nanowires-$LaPO_4$ modified carbon paste electrode. *Sens. Actuat. B* **2013,** *182*, 610-617.

41. Zhang, L.; Yuan, W. J.; Hou, B.Q. Nano-Cu/PSA III modified glassy carbon electrode for simultaneous determination of ascorbic acid, dopamine and uric acid. *J. Electroanal. Chem.* **2013,** *689*, 135-141.

42. Chih, Y. K.; Yang, M. C. An 2, 2′-azino-bis(3-ethylbenzthiazoline-6-sulfonic acid)-immobilized electrode for the simultaneous detection of dopamine and uric acid in the presence of ascorbic acid. *Bioelectrochemistry* **2013,** *91*, 44-51.

Laccase biosensor based on phytic acid modification of nanostructured SiO_2 surface for sensitive detection of dopamine

Wenbo Zhao*, Kuai Wang, Yuan Wei, Yinghui Ma, Lingling Liu,

and Xiaohua Huang*

National and Local Joint Engineering Research Center of Biomedical Functional Materials, Jiangsu Key Laboratory of Biofunctional Materials, College of Chemistry and Materials Science, Nanjing Normal University, Nanjing 210023, P. R. China.

TOC

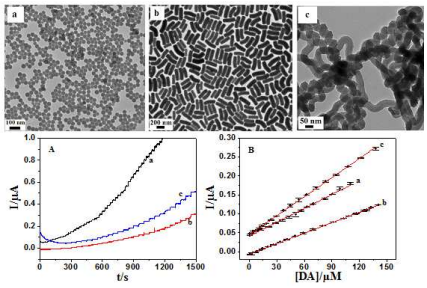

The different morphologies nanostructured silica-phytic acid (SiO_2-PA) particles were used as electrode decorated materials to achieve the sensitive detection of dopamine (DA). Compared to spherical SiO_2-PA (s-SiO_2-PA) and rod-like (r-SiO_2-PA), laccase immobilized onto helical SiO_2-PA (h-SiO_2-PA) film exhibited higher current signals and low detection limit. Results indicated that the proposed biosensor could be efficiently used for the determination of DA in pharmaceutical and human blood plasma samples.